An Analysis of a Coarse-Group Subgroup Method Based on the Physical Probability Tables in APOLLO3®

Emeline Rosier, Li Mao, Richard Sanchez, Luiz Leal, Igor Zmijarevic

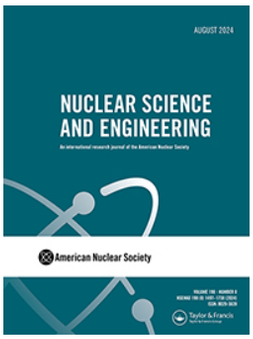

Nuclear Science and Engineering

ISSN: (Print) (Online) Journal homepage: www.tandfonline.com/journals/unse20

An Analysis of a Coarse-Group Subgroup Method Based on the Physical Probability Tables in APOLLO3®

Emeline Rosier, Li Mao, Richard Sanchez, Luiz Leal & Igor Zmijarevic

To cite this article: Emeline Rosier, Li Mao, Richard Sanchez, Luiz Leal & Igor Zmijarevic (24 May 2024): An Analysis of a Coarse-Group Subgroup Method Based on the Physical Probability Tables in APOLLO3®, Nuclear Science and Engineering, DOI: 10.1080/00295639.2024.2340143

To link to this article: https://doi.org/10.1080/00295639.2024.2340143

NUCLEAR SCIENCE AND ENGINEERING

DOI: https://doi.org/10.1080/00295639.2024.2340143

An Analysis of a Coarse-Group Subgroup Method Based on the Physical Probability Tables in APOLLO3®

Emeline Rosier,[a] Li Mao,[a]* Richard Sanchez,[a] Luiz Leal,[b†] and Igor Zmijarevic[a]

[a]*Université Paris-Saclay, CEA, Service d'Études des Réacteurs et de Mathématiques Appliquées, 91191, Gif-sur-Yvette, France*

[b]*Institut de Radioprotection et de Sûreté Nucléaire, PSN-RES/SNC/LN, Fontenay-aux-Roses, 92260, France*

Received November 17, 2023
Accepted for Publication April 1, 2024

Abstract — *The legacy subgroup method of the APOLLO3® code, denoted the SG-GR-383g method in this paper, relies on the fine structure equation solved by the means of the General Resonance model and of the mathematical probability tables (MPTs) that are computed on the fly for the resonant mixture. Because of the use of these MPTs, a fine energy structure of 383 groups has to be employed.*

In our recent work, with the intention of decreasing computational time, a subgroup method adapted to coarse-group calculations has been implemented in APOLLO3. It is based on the use of physical probability tables (PPTs), taking into account the mixture treatment, and on the Intermediate Resonance model to derive the subgroup equations, as well as the application of the Superhomogenization correction to ensure the preservation of the reaction rates in a multigroup calculation. This method, denoted SG-IR-69g in this paper, uses a 69-coarse-group energy mesh. This paper presents a comparison of the SG-IR-69g method with the legacy SG-GR-383g method, taking as reference the continuous-energy Monte Carlo TRIPOLI-4® calculations on test cases of 3 × 3 pin cells, with a central cell being either a water hole or a Gd-UO_2 pin cell surrounded by UO_2 pin cells. Similar accuracy on the multiplication factor was obtained for both the SG-GR -383g and SG-IR-69g methods, although more error compensations were found in the multigroup reaction rates of the latter. Even though the calculation of PPTs is more expensive than that of the mathematical ones, overall the SG-IR-69g method is more time efficient thanks to the decrease in the number of energy groups.

Keywords — *Subgroup methods, physical probability tables, intermediate resonance model, mathematical probability tables, general resonance model.*

Note — *Some figures may be in color only in the electronic version.*

I. INTRODUCTION

The numerical solution of the neutron transport equation can be realized with deterministic codes that require discretizing all the variables of the phase space. In particular, the energy variable is discretized with the so-called multigroup approximation, where the energy domain is sliced into energy groups inside of which neutrons are assumed to be monokinetic. The multigroup cross sections, which are employed to solve the multigroup form of the neutron transport equation, are typically prepared at a preliminary stage through the application of a nuclear data processing code that condenses the continuous-energy nuclear data evaluation into a multigroup library by using a generic weight function. In most cases, this weight function is not representative of the specific problem, especially in energy groups with the presence of cross-section resonances where neutron flux depression around resonances can be spatially dependent. Consequently, only the application of the self-shielding procedure can provide the averaged cross-section values allowing for an accurate

*E-mail: li.leimao@cea.fr
†Current Address: Oak Ridge National Laboratory, Nuclear Energy and Fuel Cycle Division, Oak Ridge, Tennessee 37831; leall-c@ornl.gov

solution of the multigroup transport equation. The global accuracy of the deterministic code therefore essentially relies on the quality of the self-shielding method.

Subgroup methods are a category of self-shielding methods relying on the use of probability tables as quadrature formula to compute group-averaged quantities, such as multigroup reaction rates. Two types of probability tables, mathematical probability tables (MPTs)[1] and physical probability tables (PPTs), are currently employed in the self-shielding methods of deterministic codes. The MPTs are generated by preserving the first powers of the neutron pointwise infinitely diluted cross sections. Without knowledge of the neutron spectrum, the use of MPTs requires a fine energy structure in order to catch the detailed spectral variation. The legacy self-shielding methods of the APOLLO2[2] and APOLLO3[3] codes employ the MPTs and require an energy mesh of 281 or 383 groups.

Contrary to the MPTs, the PPTs are obtained through preserving the physical characteristics of the system, such as dilution-dependent effective cross sections or reaction rates, which are generated by neutron slowing-down calculations in representative simplified neutron transport problems, such as infinite homogeneous media or fuel cell geometries. With knowledge of the physical characteristics, using the PPTs together with the Intermediate Resonance (IR) model requires much fewer energy groups than using the MPTs. The PPTs have been successfully employed for coarse-group calculations, with only a few tens of energy groups, obtaining good precision in lattice codes such as WIMS,[4] HELIOS,[5] DeCART,[6] nTRACER,[7] MPACT,[8] and NECP-X.[9] The DRAGON[10] code employs the PPTs without the application of the traditional IR model, therefore it still requires an energy structure of more than 100 groups.

The legacy subgroup method of the APOLLO3 code, the SG-GR-383g method,[11] relies on the fine-structure equation[11] solved by means of the General Resonance (GR) model[12] and of the mixture MPTs[13] that are computed on the fly for the resonant mixture. This method has been successfully applied to typical pressurized water reactor (PWR) calculations with a few tens of pcm (10^{-5}) of error on the multiplication factor[11] compared to a TRIPOLI-4 continuous-energy Monte Carlo reference calculation,[14] but at the price of expensive computational time.[15] The development of the Equivalent Dancoff-factor Cell method[15] has consequently led to an acceleration of the calculations while preserving equivalent precision in a typical PWR assembly calculation, but the online generation of mixture MPTs and the use of a fine energy mesh of 383 groups still leads to a prohibitively long CPU time for industrial applications.

Decreasing the number of energy groups in APOLLO3 lattice calculations is one ongoing axis of improvement to reduce the computational time, as the number of transport equation solutions in flux calculation is linearly dependent on the number of groups; hence, the interest in the use of PPTs. Recent efforts have led to the implementation in APOLLO3 of a module capable of calculating on the fly the PPTs for a resonant mixture by preserving effective cross sections in an infinite homogeneous medium (IHM).[16] Because the GR model is not suitable for coarse-group calculations, a subgroup method based on the use of the IR model[17] following the methodology presented in Refs. [9,18] has been implemented in APOLLO3. This newly implemented method, denoted SG-IR-69g in this paper, is utilized on a coarse 69-group energy mesh adapted from the energy structure available in the WIMS-D library.[19]

The objective of this paper is to analyze the accuracy and computational time of the SG-IR-69g method by comparing it with the SG-GR-383g method, taking as reference the TRIPOLI-4 continuous-energy Monte Carlo calculations. In Sec. II, a summary of the SG-GR-383g method is first presented. In Sec. III, the theory of the SG-IR-69g method is detailed. Section IV gives the results obtained with both the SG-GR-383g and SG-IR-69g methods for a benchmark composed of 3 × 3 pin cells. Section V provides the conclusions of this study.

II. A BRIEF REMINDER OF THE SG-GR-383G SUBGROUP METHOD

The current subgroup method of APOLLO3, denoted in this paper as SG-GR-383g, is based on the use of the MPTs. For a given mixture of resonant isotopes, a probability table is a discrete set of parameters $\{\omega_k^g, \sigma_k^g, \sigma_{\rho,x,k}^g, k = 1, ..., K\}$, where g is the energy group index and k is the subgroup index, with K being the order of the probability table. ω_k is the weight associated with the subgroup total cross section σ_k^g of the mixture and the subgroup partial cross sections for reaction ρ (absorption, scattering, etc.) and resonant isotope x, $\sigma_{\rho,x,k}^g$.

This subgroup method is based on the solution of the following fine-structure equation[11]:

$$\Sigma_i(u)V_i\phi_i(u) = \sum_j P_{ij}(u)V_j\Big(N_{0,j}r_{0,j}\phi_j(u) + \Sigma_{1,s,j}(u)\Big) \quad , \tag{1}$$

where

i, j = region indexes

0, 1 = resonant and moderator mixtures, respectively,

Σ, Σ_s = total and scattering macroscopic cross sections

P_{ij} = probability for a neutron born uniformly and isotropically in region j to first collide in a region i

N = number density

V = volume

ϕ = fine-structure factor

$r\phi$ = resonant scattering source.

Equation (1) is derived from the collision probability formalism of the neutron transport equation with the application of the fine-structure assumption.[20]

According to the fine-structure assumption, for a lethargy u in an energy group g and for a given region i, the neutron flux $\Phi_i(u)$ is approximated as follows:

$$\Phi_i(u) = \chi_i(u)\phi_i(u) \quad , \tag{2}$$

$$r_{0i}[\chi_i(u)\phi_i(u)] \approx \chi_i(u) r_{0i}\phi_i(u) \quad , \tag{3}$$

$$\chi_i(u) = \chi(u) \quad , \tag{4}$$

where χ is called the macroscopic flux, varying smoothly in space, and ϕ is the fine-structure factor containing the resonant part of the neutron flux. Next, the GR model[12] is employed to approximate the resonant scattering sources,

$$r_0\phi(u) \approx \langle r_0\phi\rangle^{GR,g} = \sum_{x\in \text{res}} \sum_{g'} a_x p_x^{g'\to g} \langle \tau_{s,x}\rangle^{g'} \quad , \tag{5}$$

where $p_x^{g'\to g}$ is the probability for a neutron to scatter from group g' to g after its collision on the resonant isotope x, and

$$\langle \tau_{s,x}\rangle^g = \frac{1}{\Delta u^g} \int_g \sigma_{s,x}(u)\phi^{GR}(u) du \tag{6}$$

is the group-averaged scattering reaction rate. The subgroup equation, derived from the multigroup formalism of the fine-structure equation [Eq. (1)] and from the GR model [Eq. (5)], is solved by the Improved Direct Method[21] to retrieve the subgroup flux in every spatial region,

$$\left[\Sigma_{1,i}^g + N_{0,i}\sigma_k^g\right] V_i \phi_{i,k}^g = \sum_j P_{ij,k}^g V_j N_{0,j} \left[\sum_{x\in \text{res}} a_x p_x^{g\to g} \sum_{l=1}^{K} \omega_l^g \sigma_{s,x,l}^g \phi_{j,l}^g + \sum_{g'\neq g} \langle r_0\phi\rangle_j^{g'\to g} + \Sigma_{1,s,j}^g \right] . \tag{7}$$

The "Superhomogenization" (SPH) correction[11] is then applied to the multigroup cross sections by preserving the reference reaction rates of the preceding subgroup solution. The subgroup parameters appearing in Eq. (7) are related to the mixture MPTs traditionally used in the APOLLO3 self-shielding methods. They are generated on the fly by the GALILEE nuclear data processing system[22] employing the CALENDF methodology,[23] and require the use of a fine energy discretization of 383 groups to accurately account for the neutron energy spectrum. This 383-group energy mesh is a refinement of the legacy SHEM-281 energy mesh,[24] with the introduction of additional groups in the resolved resonance energy domain, as proposed in Ref. [25].

III. THEORY OF THE SG-IR-69G SUBGROUP METHOD

III.A. Overview of the Method

This coarse-group subgroup method employs a 69-group energy mesh adapted from the energy structure available in the WIMS-D library,[19] with the group boundaries adjusted to those of the MUSCLET energy mesh composed of 23 317 groups.[26] For such a coarse energy mesh, the GR model is no more suitable, instead, the IR model[17] is applied to approximate the resonant and moderator scattering sources of the elastic slowing-down equation. For an isotope x in an energy group g, the IR scattering operator is written as

$$R_x^{IR}\Phi^g = N_x\left[\lambda_x^g \sigma_{p,x}^g + (1-\lambda_x^g)\sigma_{s,x}^g \Phi^g\right] \quad , \tag{8}$$

where N_x, $\sigma_{p,x}$ and $\sigma_{s,x}$ are the number density, the microscopic potential, and the scattering cross sections, respectively. λ_x^g is the Goldstein-Cohen parameter, or the IR parameter, which is not contained in the multigroup libraries destined for APOLLO3 lattice calculations, and consequently, has to be evaluated for the SG-IR-69g method. Currently, the IR parameters are computed for every isotope of interest by the means of Monte Carlo

calculations using the TRIPOLI-4 code following the procedure described in Ref. [27].

The SG-IR-69g method requires the PPTs for the subgroup computation. We decided to deal with the resonance interference of resonant isotopes by employing the mixture PPTs. In order to evaluate the mixture PPTs, the per-isotope MPTs on the MUSCLET energy mesh are read from the APOLLO3 library. Then, for each resonant mixture, the on-the-fly calculation of the 23 317-group mixture MPTs is carried out by the TREND-PT module provided by the GALILEE project.[22] After that, the IHM ultra-fine-group (UFG) slowing-down calculation is performed for each resonant mixture with a set of dilutions. The obtained mixture effective cross sections at different dilutions allow for the subsequent generation of the mixture PPTs.

The major calculation steps of the SG-IR-69g subgroup method are listed in the following:

1. The on-the-fly calculation of the 23 317-group mixture MPTs.

2. The IHM UFG slowing-down calculation to compute the reference effective cross sections of the resonant mixture for a set of dilutions.

3. The mixture PPT generation by preserving the reference IHM cross sections.

4. The IR-based subgroup equation is solved using the mixture PPTs, and the SPH correction is applied in order to retrieve multigroup cross sections through reaction rate preservation.

The interested reader can refer to Ref. [12] for the calculation of mixture MPTs from per-isotope MPTs, which will not be discussed here. The remaining steps are detailed in the subsequent subsections.

III.B. IHM UFG Slowing-Down Calculation

The APOLLO3 legacy UFG-IHM solver solves the fine-structure equation [Eq. (1)] applied to an IHM on the finest energy structure available in the APOLLO3 multigroup libraries, namely, the MUSCLET energy mesh composed of 23 317 groups.[26] In an IHM consisting of a mixture of resonant isotopes and a pseudo hydrogen (H1) isotope that has only potential scattering, Eq. (1) divided by the density of resonant isotopes reads

$$\left[\sigma_0(u)+\sigma_{b,h}\right]\phi(u)=r_0\phi(u)+\sigma_{b,h}\quad , \tag{9}$$

where $\sigma_{b,h}=a_h\sigma_{p,h}$ is the background dilution of the medium and a_h is the proportion of a H1 isotope in the mixture. We remark that, in the right side of this equation, the contribution of the moderator to the sources is a constant equal to $\sigma_{b,h}$, while the resonant operator is approximated with the GR model [Eq. (5)].

Defining the external scattering source from other groups to a fine energy group g as

$$S^g_{ext}=\sum_{g'\neq g}\sum_{x\in\text{res}}a_x\,p_x^{g'\to g}\langle\tau^{GR}_{s,x}\rangle^{g'}+\sigma_{b,h}\quad , \tag{10}$$

we derive the expression of the fine-structure equation of the legacy UFG IHM solver of APOLLO3 as

$$\left[\sigma_0(u)+\sigma_{b,h}\right]\phi(u)=S^g_{ext}+\sum_{x\in\text{res}}a_x\,p_x^{g\to g}\langle\tau^{GR}_{s,x}\rangle^{g}\quad . \tag{11}$$

From Eqs. (5), (6), and (11), the expression of the averaged scattering rate of isotope x is derived as

$$\langle\tau^{GR}_{s,x}\rangle^g=\frac{S^g_{ext}}{\mu^g}\,I^g_{s,x}\quad , \tag{12}$$

where we define the following quantities:

$$I^g_{s,x}=\int_g\frac{\sigma_{s,x}(u)}{\sigma_0(u)+\sigma_{b,h}}du \tag{13}$$

$$\mu^g=\Delta u^g-\sum_{x\in\text{res}}a_x\,p_x^{g\to g}I^g_{s,x}\quad . \tag{14}$$

The integral appearing in Eq. (13) is computed using the mixture MPTs as quadrature formula.

Let us note that the multigroup solution is computed from higher to lower energy groups. The downscattering sources are therefore known; but the upscattering sources from the lower energy groups g', $g'>g$, are unknown when group g is being considered. In this case the Statistical (ST) model[21] has to be employed to evaluate the upscattering sources. It is a special case of the GR model where the transfer probabilities are zero if $g'\neq g$ and equal to one otherwise. A similar analysis provides the expression of the ST-based scattering rate,

$$\langle\tau^{ST}_{s,x}\rangle^{g'}=I^{g'}_{s,x}\frac{\sigma_{b,h}}{\Delta u^{g'}-\sum\limits_{x\in\text{res}}a_xI^{g'}_{s,x}}\quad , \tag{15}$$

which is employed instead of Eq. (12) when $g'>g$. Once all the scattering sources have been evaluated, they are injected into Eq. (11) to obtain the expression of the

neutron fine-structure factor $\phi^{GR}(u)$, which is integrated over the range of a fine group to retrieve the multigroup solution and replaced in the expression of the multigroup reaction rates

$$\phi^g = \int_g \phi^{GR}(u)du \quad , \tag{16}$$

$$\tau^g_{\rho,x} = \int_g \sigma_{\rho,x}(u)\phi^{GR}(u)du \quad , \tag{17}$$

for each partial reaction ρ. The mixture MPTs are once again employed to compute these multigroup quantities. The effective cross sections of the resonant mixture are then obtained by condensing the contribution of each fine group g to the coarse-group G it belongs to,

$$\sigma^G_{\rho,x} = \frac{\sum_{g\in G} \tau^g_{\rho,x}}{\sum_{g\in G} \phi^g} \quad . \tag{18}$$

In our recent work,[28] it was noticed that the legacy fine-structure solver provided satisfying results in the case of a single isotope. However, in the case of a uranium mixture, the maximum error on the ^{235}U absorption cross section can reach 15%. To remedy this accuracy issue, an improved UFG IHM solver[29] based on the slowing-down equation, without the application of the fine-structure approximation, was recently developed. This slowing-down solver considers the same IHM composed of the resonant mixture diluted with a H1 isotope, denoted h with proportion a_h, whose only non-null cross section is the potential scattering one, $\sigma_{p,h}$. This H1 isotope contributes to the scattering sources, leading to the following slowing-down equation:

$$\left[\sigma_0(u) + a_h\sigma_{p,h}\right]\Phi(u) = r_0\Phi(u) + a_h r_h\Phi(u) \quad . \tag{19}$$

Both the resonant and the moderator scattering sources are approximated with the GR model so that the moderator source for a lethargy u in a UFG g is not a constant anymore and is more accurately calculated with

$$r_h\Phi(u) \approx \langle r_h\Phi^{GR}\rangle^g = \sum_{g'} p_h^{g'\to g}\langle\tau^{GR}_{s,h}\rangle^{g'} \quad . \tag{20}$$

The final form of the improved UFG IHM slowing-down equation in a fine group g becomes

$$\left[\sigma_0(u) + a_h(1-p_h^{g\to g})\sigma_{p,h}\right]\Phi(u) = S^g_{\text{ext}} + \sum_{x\in\text{res}} a_x\, p_x^{g\to g}\langle\tau^{GR}_{s,x}\rangle^g \quad , \tag{21}$$

where S^g_{ext} is the external scattering source, whose expression is given by

$$S^g_{\text{ext}} = \sum_{g'\neq g}\sum_{x\in\text{res}} a_x\, p_x^{g'\to g}\langle\tau^{GR}_{s,x}\rangle^{g'} + \sum_{g'<g} a_h\, p_h^{g'\to g}\langle\tau^{GR}_{s,h}\rangle^{g'} \quad . \tag{22}$$

A comparison of Eqs. (11) and (21) provides the expression of the background dilution associated with this improved formalism,

$$\sigma_b = a_h\left(1-p_h^{g\to g}\right)\sigma_{p,h} \quad . \tag{23}$$

The enhanced UFG IHM equation [Eq. (21)] is solved in a similar way as the legacy fine-structure equation.

Our numerical results[29] show that with the slowing-down UFG IHM solver, in the case of a uranium mixture, the maximum error on the ^{235}U absorption cross section is reduced from 15% to less than 1%. This proves that the assumption of a constant moderator scattering source, due to adopting the fine-structure assumption equaling to $\sigma_{b,h}$ in Eq. (9), is erroneous in the vicinity of a large resonance. The largest errors have been found located in groups containing the ^{238}U largest resonances.

III.C. On-the-Fly Calculation of the Mixture PPTs

The calculation of the mixture PPTs of order K is a fitting procedure that requires the on-the-fly tabulation of the effective cross sections of the resonant mixture $\{\overline{\sigma}^g(\sigma_{b,m}), \overline{\sigma}^g_{res}(\sigma_{b,m}), \overline{\sigma}^g_{\rho,x}(\sigma_{b,m}), m = 1, ..., M\}$ for at least $M \geq 2K-1$ values of background dilutions σ_b, one of them being $\sigma_b = 1\times10^{10}$ barns, considered as infinite. Given a set of M background dilutions, the corresponding effective cross sections are obtained by using the improved UFG IHM slowing-down solver previously presented.

In a preliminary implementation of the PPTs inside of the APOLLO3 code, the fitting procedure aimed to preserve the total cross section of the resonant mixture using a rational fraction, whose coefficients have to be determined, as described in Ref. [30]. But this led to poor results when combined with the IR-based subgroup equations, which are detailed in the next subsection. A recent work by Liu and al.[18] showed that the fitting of the

resonant cross section is a better choice in the prospect of solving IR-based equations, with the resonant cross section being defined as

$$\sigma_{res}^{g} = \sum_{x \in \text{res}} a_x \left[\sigma_{a,x}^{g} + \lambda_x^{g} (\sigma_{s,x}^{g} - \sigma_{p,x}) \right] \quad , \tag{24}$$

where $\sigma_{p,x}$ is the potential cross section of isotope x, and λ_x^g is its Goldstein-Cohen parameter. To justify this choice, one can consider that the IR solution of an IHM composed of a resonant mixture and of a H1 h will be derived in the form of

$$\Phi^{IR}(u) = \frac{\sigma_b^{IR}}{\sigma_{res}^{IR}(u) + \sigma_b^{IR}} \quad , \tag{25}$$

where the expression of the dilution incorporates the use of the IR model,

$$\sigma_b^{IR} = a_h \sigma_{p,h} + \sum_{x \in \text{res}} a_x \lambda_x \sigma_{p,x} \quad . \tag{26}$$

Therefore, the fitting with the resonant cross section can be considered as IR fitting since it is consistent with the IR IHM solution. If we were to set all IR parameters to 1, the IR model would be degraded to the Narrow Resonance (NR) model, resulting in

$$\Phi^{NR}(u) = \frac{\sigma_b^{NR}}{\sigma_{res}^{NR}(u) + \sigma_b^{NR}} \quad , \tag{27}$$

$$\sigma_{res}^{NR}(u) = \sigma_t(u) - \sum_{x \in \text{res}} a_x \sigma_{p,x} \quad , \tag{28}$$

$$\sigma_b^{NR} = a_h \sigma_{p,h} + \sum_{x \in \text{res}} a_x \sigma_{p,x} \quad . \tag{29}$$

Consequently, from Eqs. (27), (28), and (29) for the NR IHM solution, the fitting with the total cross section is not consistent even with the NR model. This explains why the PPTs computed by the fitting of the total cross section do not lead to satisfying results.

As proposed in Sec. 4.2.4 of Ref. [30], the fitting of the resonant cross section is operated through the computation of the unknown coefficients of the following rational fraction:

$$\overline{\sigma}_{res}^{g}(\sigma_{b,m}) = \frac{c_0^g + c_1^g \sigma_{b,m} + c_2^g \sigma_{b,m}^2 + \ldots + c_{K-1}^g \sigma_{b,m}^{K-1}}{d_0^g + d_1^g \sigma_{b,m} + d_2^g \sigma_{b,m}^2 + \ldots + d_{K-1}^g \sigma_{b,m}^{K-1}}, \quad m = 1, \ldots, M \quad , \tag{30}$$

where $c_{K-1}^g = \overline{\sigma}_{res}^{g}(\infty)$ and $d_{K-1}^g = 1$ in order to preserve the resonant cross section for an infinite dilution. Writing Eq. (30) for all of the M values of dilutions, a linear system of equations is obtained and solved using the QR factorization of the LAPACK Fortran library.[31] A similar procedure is applied to approximate the partial cross sections (including the total, absorption, scattering, and fission reactions) as rational fractions, using the same denominator as in Eq. (30),

$$\overline{\sigma}_{\rho,x}^{g}(\sigma_{b,m}) = \frac{e_0^g + e_1^g \sigma_{b,m} + e_2^g \sigma_{b,m}^2 + \ldots + e_{K-1}^g \sigma_{b,m}^{K-1}}{d_0^g + d_1^g \sigma_{b,m} + d_2^g \sigma_{b,m}^2 + \ldots + d_{K-1}^g \sigma_{b,m}^{K-1}}, \quad m = 1, \ldots, M \quad , \tag{31}$$

where $e_{K-1}^g = \overline{\sigma}_{\rho,x}^{g}(\infty)$ in order to preserve the partial cross section for an infinite dilution. The parameters of the PPT, namely, the subgroup weights and cross sections, are deduced from the coefficients of the rational fractions. First, the subgroup resonant cross sections $\sigma_{res,k}^g$ are the roots of the following polynomial:

$$\begin{aligned} P(-\sigma_{res}) = {} & c_0^g + (c_1^g + d_0^g)(-\sigma_{res}) + \ldots \\ & + (c_{K-1}^g + d_{K-2}^g)(-\sigma_{res})^{K-1} \\ & + (-\sigma_{res})^{K} \quad . \end{aligned} \tag{32}$$

The Aberth method[32] is employed to find simultaneously all the roots, before checking that they are real and positive. If this is the case, the subgroup weights are obtained with the relation

$$\omega_k^g = \frac{d_0^g + \ldots + d_{K-2}^g (-\sigma_{res,k}^g)^{K-2} + (-\sigma_{res,k}^g)^{K-1}}{\prod_{l \neq k} (\sigma_{res,l}^g - \sigma_{res,k}^g)}, \quad k = 1, \ldots, K \quad , \tag{33}$$

and the subgroup partial cross sections, including the total cross section, are computed with

$$\sigma_{\rho,x,k}^g = \frac{\sum_{l=0}^{K-1} e_l^g (-\sigma_{res,k}^g)^l}{\sum_{l=0}^{K-1} d_l^g (-\sigma_{res,k}^g)^l}, k = 1, \ldots, K \quad . \tag{34}$$

If one or more of the roots of Eq. (32) is found to be either negative or complex, then the fitting procedure of the effective cross sections is restarted with a decreased PPT order $K' = K - 1$.

At the end of this procedure, homogeneous PPTs are obtained. The computation of heterogeneous PPTs, based on the preservation of the solutions of the UFG pinwise slowing-down equation,[33] has been ruled out because it has been estimated to be too time expensive to fit the purpose of on-the-fly calculations.

III.D. IR-Based Subgroup Equations

The use of the IR model [Eq. (8)] in the elastic slowing-down equation leads to the following equation for a subgroup k in an energy group g:

$$\left[\Sigma^g_{1,i} + \sum_x N_{x,i}\sigma^g_{x,k,i}\right] V_i \Phi^g_{k,i} = \sum_j V_j P^g_{ij,k} R^{IR}_j \Phi^g_{k,j} \quad , \tag{35}$$

where i and j are region indexes, V is a volume, and P_{ij} is the collision probability. Σ_1 represents the macroscopic total cross section of the moderator; that is to say all the isotopes in the mixture except the resonant ones. N_x is the number density of isotope x in the resonant mixture, and $\sigma_{x,k}$ is its microscopic total cross section associated with subgroup k. $R^{IR}_j \Phi^g_{k,j}$ is the IR scattering source for a region j, which is the sum of the contributions coming from the moderator source, and in the case of a resonant region, also the resonant sources,

$$R^{IR}_j \Phi^g_{k,j} = \sum_{x\in \text{res}} N_{x,j}\left[(1-\lambda^g_x)\sigma^g_{s,x,k,j}\Phi^g_{k,j} + \lambda^g_x \sigma^g_{p,x}\Delta u^g \omega^g_k\right] + \sum_{x\in \text{mod}} N_{x,j}\left[(1-\lambda^g_x)\sigma^g_{s,x,j}\Phi^g_{k,j} + \lambda^g_x \sigma^g_{p,x}\Delta u^g \omega^g_k\right] \quad . \tag{36}$$

Equation (35) forms a linear system of equations that is solved for the subgroup flux in every region for a given energy group. The latter is used to compute the self-shielded cross sections for resonant isotopes for a given reaction ρ using the previously computed subgroup parameters of the PPT of order K,

$$\sigma^g_{\rho,x,i} = \mu^g_i \times \frac{\sum_{k=1}^{K} \omega^g_k \sigma^g_{\rho,x,k,i}\Phi^g_{k,i}}{\sum_{k=1}^{K} \omega^g_k \Phi^g_{k,i}} \quad . \tag{37}$$

where μ^g_i is the SPH factor computed through an iterative equivalence procedure enforcing that the solution of the multigroup problem

$$\Sigma^g_i V_i \Phi^g_i = \sum_j V_j P^g_{ij} R^{IR}_j \Phi^g_j \tag{38}$$

yields the same reaction rates as the ones from the subgroup equation [Eq. (35)], which are considered to be the reference rates to be preserved. In this work, the μ^g_i SPH factor is calculated in every region i and resonant group g according to the procedure described in Ref. [18], which was inspired from the work of Ref. [34].

IV. NUMERICAL RESULTS

Two benchmarks defined with motifs of 3 × 3 cells have been selected for the numerical comparison of the SG-GR -383g and of the SG-IR-69g methods. All the outer cells of the motifs are typical UO_2 pin cells with an enrichment of about 3.7%, while the central cell is either a water hole or a Gd-UO_2 pin cell. The Gd-UO_2 fuel corresponds to an enrichment of 4.0 wt% in ^{235}U and 10.0 wt% in Gd_2O_3. The dimensions and compositions of the different materials are taken from the Yamamoto et al. benchmark.[35]

The self-shielding procedure is followed by a transport calculation, based on the Two and three Dimensional Transport solver (TDT) unstructured geometry method of characteristics (MOC) flux solver of APOLLO3.[36] The tracking parameters were set to 32 azimuthal angles, four polar angles, and a transversal integration step of 0.01 cm. The anisotropic scattering order was fixed to P3. Because of the symmetry of the geometry of the 3 × 3 cluster of cells, the calculation was carried out on a reduced geometry, shown in Figs. 1 and 2, with reflective boundary conditions. For the self-shielding calculation, the fuel pins were divided into 10 rings corresponding to percentages of 20, 20, 10, 10, 10, 10, 5, 5, 5, and 5, respectively, of the total fuel volume. For the flux calculation, each ring was divided into eight additional sectors.

The results obtained with the 383-group GR-based subgroup method (SG-GR-383g) and with the 69-group IR-based subgroup method (SG-IR-69g) were compared with the reference TRIPOLI-4 value. For a meaningful comparison, both the SG-GR-383g and the SG-IR-69g calculations, as well as the reference continuous-energy calculations of TRIPOLI-4, employed the library based on the JEFF-3.1.1[37] nuclear data evaluation. The self-shielding range of the SG-GR-383g method was from

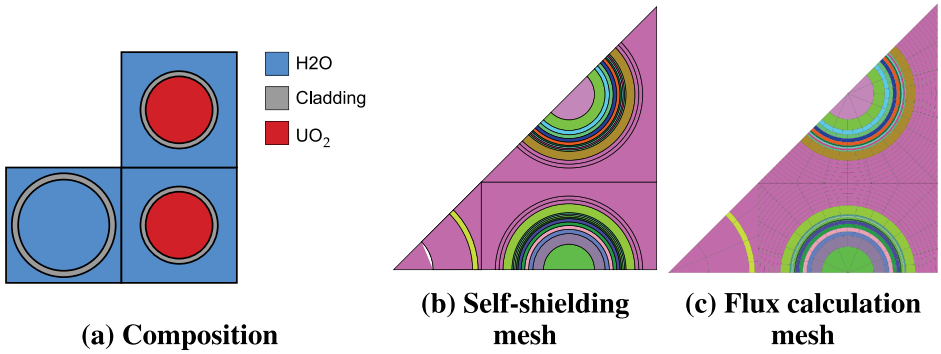

Fig. 1. Motif of 3 × 3 cells with a central water hole.

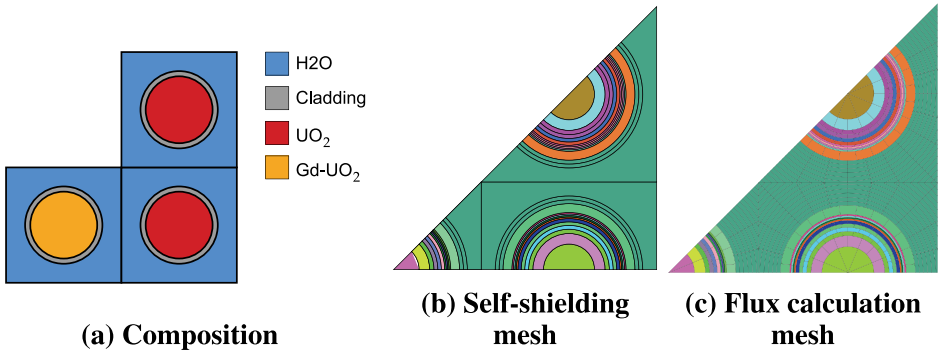

Fig. 2. Motif of 3 × 3 cells with a central Gd-UO_2 cell.

0.55549 eV to 111.535 keV, while the one for the SG-IR -69g method was from 2.0711 eV to 9.1188 keV. This latter range was limited by the IR parameters λ^g that for now have not been computed for lower or higher energy.

Table I displays the differences in the multiplication factor k_{eff} obtained with the SG-GR-383g and SG-IR-69g calculations and the reference TRIPOLI-4 value. This error is on the order of tens of pcm for the SG-GR-383g method and of a hundred pcm for the SG-IR-69g method in the case of the central water hole. It can be observed that the addition of the Gd-UO_2 fuel pin in the central cell, in the second configuration of the benchmark, leads to a slight increase in the error on the k_{eff} for the SG-GR-383g method, while it improves the precision of the SG-IR-69g method.

Figures 3 and 4 show the error (in percent) on the absorption and production rates, respectively, of the UO_2 resonant mixture in every pin cell of the 3 × 3 motif with the central guide tube. This error was calculated on the reaction rates integrated over the whole energy domain. The SG-GR-383g method displays a very satisfying accuracy, with less than 0.05% of difference compared to the reference Monte Carlo values in all the pin cells for both the total absorption rate and the total production rate. The

TABLE I

Difference of k_{eff} in the 3 × 3 Pin Cell Benchmarks

Method	With Central Water Hole		With Central Gd-UO_2 Cell	
	k_{eff}	Δk_{eff} (pcm)	k_{eff}	Δk_{eff} (pcm)
TRIPOLI-4®	1.46014 ± 3 pcm	–	1.13558 ± 3 pcm	–
SG-GR-383g	1.46057	43	1.13630	72
SG-IR-69g	1.45891	−123	1.13598	40

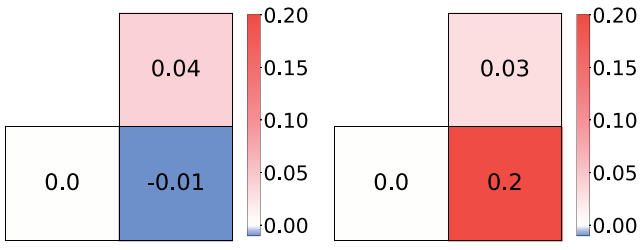

(a) SG-GR-383g **(b) SG-IR-69g**

Fig. 3. Error (in percent) for the absorption rate of the resonant mixture in the central water hole benchmark.

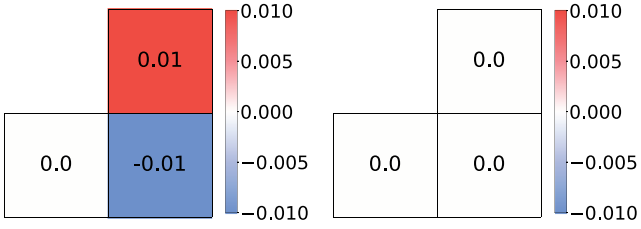

(a) SG-GR-383g **(b) SG-IR-69g**

Fig. 4. Error (in percent) for the production rate of the resonant mixture in the central water hole benchmark.

precision of the SG-IR-69g method is of the same order of magnitude, except for the absorption rate of the pin cell in the bottom-right corner, which displays a larger error of 0.2%.

This overestimation of the absorption explains the negative discrepancy on the multiplication factor evidenced in Table I, as more neutrons are absorbed. The ^{238}U isotope is the main contributor to the absorption of the UO_2 mixture. The error (in percent) in its absorption rate in each pin cell is shown in Fig. 5. When employing the SG-IR-69g method, the error in the bottom-right corner cell reaches almost 1%, which is three times more than the other cells, and what is obtained with the SG-GR-383g method. Figure 6 shows the discrepancy of the production rate of the ^{235}U isotope, which mainly contributes to the total production rate. A similar accuracy was reached with both the SG-GR-383g and the SG-IR-69g methods, but with opposite signs.

Figure 7 details the errors, displayed here in pcm in order to show the error contribution of each group to the global multiplication factor error, of both the total absorption rate and the total production rate in the bottom-right cell, where the larger errors have been observed. To simplify the comparison between the SG-GR-383g and the SG-IR-69g methods, the multigroup rates on the 383-group energy structure have been condensed into the 69-group energy mesh. One can notice that the SG-IR-69g displays the largest errors in the lower part of the resonant energy domain, which are partially compensated because of the opposite signs in different energy groups. Such fluctuations show that there are still some calibrations to be done on the SG-IR-69g method; for example, in the calculation of the IR parameters per isotope λ_x^g. The SG-GR-383g method also presents errors on the order of a few tens of pcm in some resonant energy groups, although the condensation procedure to obtain the results for the 69-group energy structure tends to flatten this type of fluctuation by the same compensation phenomenon.

Figures 8 and 9 show the error for the total absorption rate and for the total production rate in every cell of the motif of 3 × 3 pin cells, with the central cell being a Gd-UO_2 pin cell. As for the benchmark with the central guide tube, the rates presented in these figures have been integrated over the whole energy domain to display the spatial discrepancy. It can be seen that the errors for the SG-GR-383g method remain of the same order of magnitude as in the case of the central water hole benchmark, if not slightly accentuated. In the SG-IR-69g method, the errors in the outer cells are of the same order of magnitude as previously; however, the errors for the absorption

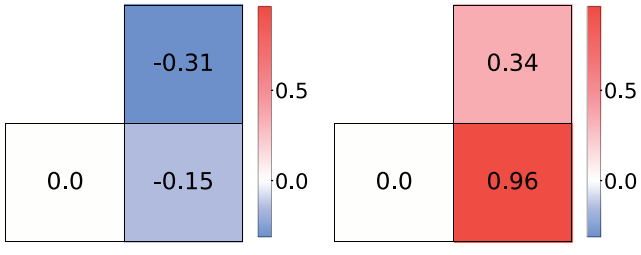

(a) SG-GR-383g **(b) SG-IR-69g**

Fig. 5. Error (in percent) for the absorption rate of the ^{238}U isotope in the central water hole benchmark.

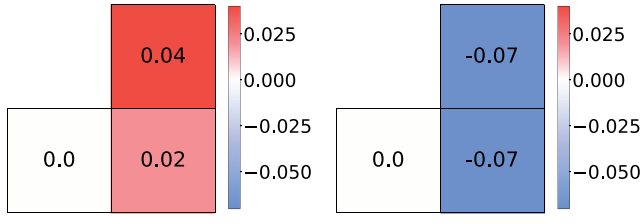

(a) SG-GR-383g **(b) SG-IR-69g**

Fig. 6. Error (in percent) for the production rate of the ^{235}U isotope in the central water hole benchmark.

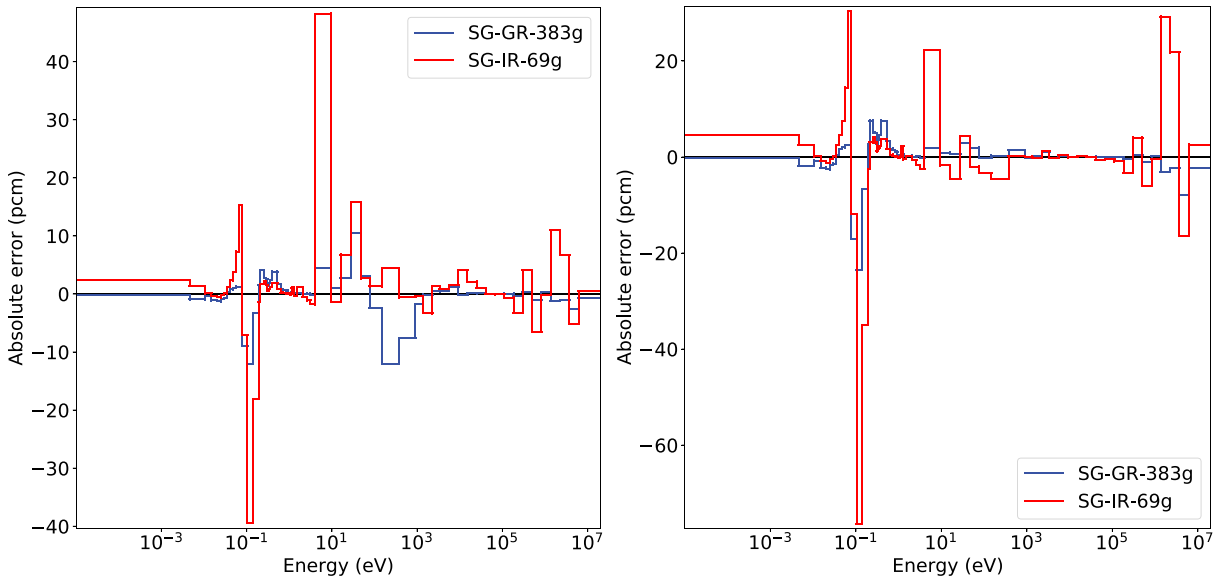

(a) Total absorption **(b) Total production**

Fig. 7. Error (in pcm) for the reaction rates of the resonant mixture in the bottom-right cell of the central water hole benchmark.

and production rates of the central Gd-UO_2 mixture are much higher, with a more than 0.6% difference compared to the reference TRIPOLI-4 value. The good accuracy on the multiplication factor observed in Table I is due to the difference in the sign of the errors in the outer and inner cells, leading to compensation effects.

Figures 10 and 11 detail the errors in each cell for the ^{238}U absorption rate and for the ^{235}U production rates, respectively. One can notice that the absorption rate of ^{238}U in the central cell is actually overestimated; the underestimation of the total absorption rate in this specific pin cell is therefore due to the other isotopes of the resonant mixture, namely, the gadolinium isotopes. These isotopes display resonances in their absorption cross sections below the energy range that is currently being self-shielded with the SG-IR-69g method because we are missing the IR parameters to run such calculations below 2 eV for now. Once the IR parameters are computed, we estimate that performing the self-shielding calculations below 2 eV will improve the accuracy in this domain. The production rate of ^{235}U in the central

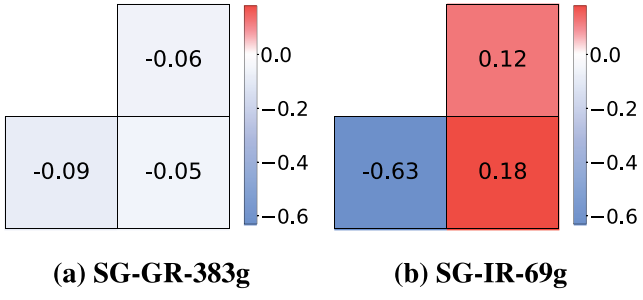

(a) SG-GR-383g **(b) SG-IR-69g**

Fig. 8. Error (in percent) for the absorption rate of the resonant mixture in the central Gd-UO_2 cell benchmark.

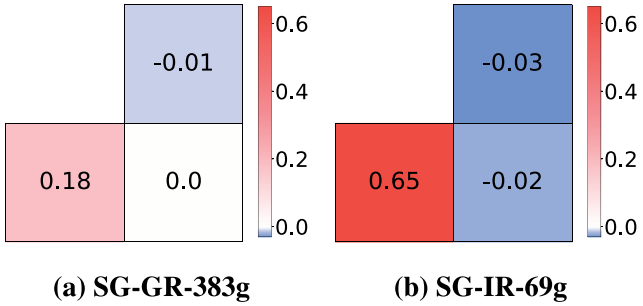

(a) SG-GR-383g **(b) SG-IR-69g**

Fig. 9. Error (in percent) for the production rate of the resonant mixture in the central Gd-UO_2 cell benchmark.

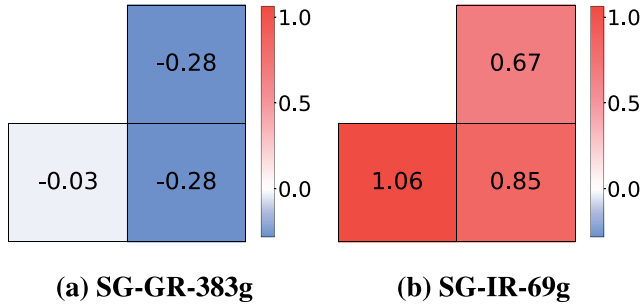

(a) SG-GR-383g **(b) SG-IR-69g**

Fig. 10. Error (in percent) for the absorption rate of the ^{238}U isotope in the central Gd-UO_2 cell benchmark.

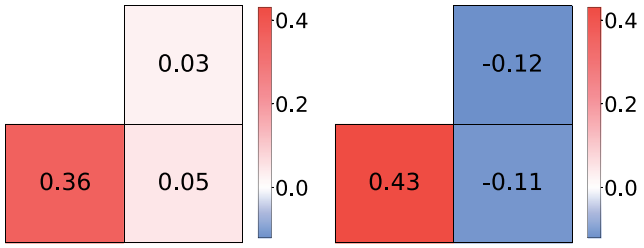

(a) SG-GR-383g **(b) SG-IR-69g**

Fig. 11. Error (in percent) for the production rate of the ^{235}U in the central Gd-UO_2 cell benchmark.

pin cell is also significantly overestimated for both self-shielding methods, with a more than 0.3% error for the SG-GR-383g method and a 0.4% error for the SG-IR-69g method.

Figure 12 details the errors, in pcm, of the multigroup total absorption rates and multigroup total production rates in the central Gd-UO_2 pin cell on the 69-group energy structure. The same large peaks are observed in the resonant domain for both methods as in the previous benchmark, where the resonant mixture was just composed of UO_2 fuel. As the ^{238}U and ^{235}U isotopes responsible for these errors are also present in the Gd-UO_2 mixture, it makes sense that their contribution to the total error is still noticeable. Significant errors can be noticed above 10 eV, and are due to the gadolinium isotopes.

Finally, the calculation time for both benchmarks and both methods is displayed in Table II. The table details the time spent on the self-shielding calculation, including the on-the-fly generation of the mixture probability table and the solution of the subgroup equations, and in the flux calculation (parallelized with OpenMP technology on 32 threads).

For the SG-GR-383g method, the time spent on the calculation of the probability tables was strictly related to the calculation of the mixture MPTs, whereas in the SG-IR-69g method it included the on-the-fly calculation of the mixture MPTs, the UFG IHM slowing-down calculations, and finally, the generation of the mixture PPTs. Therefore, it makes sense that the time spent on the probability table calculation using the SG-IR-69g was almost four times as much as the one for the SG-GR -383g in the benchmark with the central water hole.

However, the time spent on the subgroup calculation by the SG-IR-69g method was reduced by a factor of 18 compared with that by the SG-GR-383g method. Consequently, when considering the total time in self-shielding calculation, that is, the probability table and the subgroup calculations, the difference in time between the SG-IR-69g and the SG-GR-383g is narrowed down to less than 2. And finally, when considering the global transport calculation, including both the self-shielding and the flux calculations, the use of the SG-IR-69g leads to a reduction in computational time of a factor almost 3.

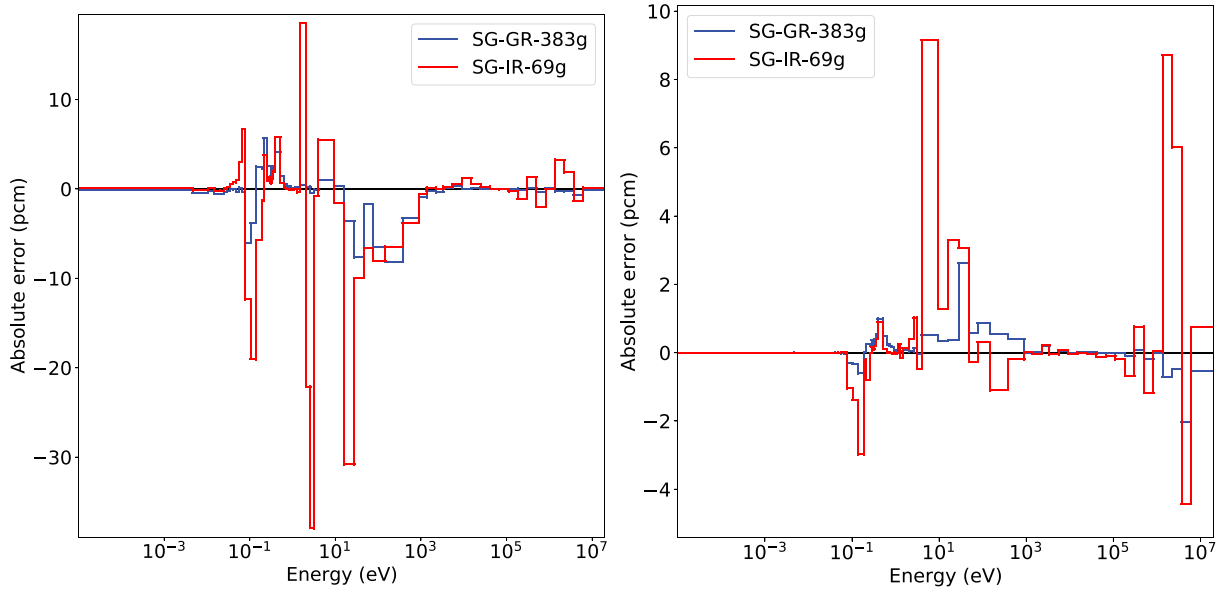

(a) Total absorption **(b) Total production**

Fig. 12. Error (in pcm) for the reaction rates of the resonant mixture in the central cell of the central Gd-UO_2 cell benchmark.

TABLE II

CPU Time in Seconds

	With Central Water Hole			With Central Gd-UO_2 Cell		
	Self-Shielding			Self-Shielding		
	Probability Table	Subgroup	Flux	Probability Table	Subgroup	Flux
SG-GR-383g	1.5	1.8	57.8	4.8	6.2	51.2
SG-IR-69g	5.7	0.1	15.8	13	0.2	14.8

Let us remark that the geometry of the benchmarks presented in this paper is rather small, meaning that most of the self-shielding procedure was spent in the mixture probability table calculation. On larger geometries, such as a 17 × 17 assembly, if the number of resonant mixtures remains the same and the computational cost of solving the subgroup equations becomes dominant, the SG-IR-69g method decreases the self-shielding time by a factor of 25, as noticed in our previous work.[28]

When the number of resonant mixture for which mixture probability tables have to be calculated increases, as is the case in the central Gd-UO_2 cell benchmark, the difference in computational time between the MPT and the PPT calculations decreases. This can be explained by the fact that the number of resonant isotopes in the Gd-UO_2 medium is eight instead of two in the UO_2 medium, so the time spent in the mixture MPT calculation will be much longer, therefore becoming much more dominant in the PPT calculations.

In this motif of 3 × 3 cells benchmark, most of the global calculation time is spent in the flux calculation and not in the self-shielding calculation. In this aspect, the SG-IR-69g method performs much better than the SG-GR-383g simply because of the decrease in the number of energy groups from 383 down to 69.

V. CONCLUSIONS

In this paper, a coarse-group subgroup method, the SG-IR-69g method, recently implemented in the APOLLO3 lattice code was presented. First, the mixture MPTs of the resonant mixture were computed on the fly and used in an UFG IHM slowing-down equation solver to tabulate the reference 69-group cross sections of the mixture for a set of background dilutions. The mixture PPTs are then computed by preserving these effective cross sections. After that, the solution of the subgroup equations was obtained using the formalism of the IR model to approximate the scattering sources. Finally, the SPH correction was applied to the multigroup cross sections to ensure the conservation of the reaction rates in a multigroup calculation.

This paper assessed the SG-IR-69g method on two benchmarks made of 3 × 3 UO_2 pin cells, with a central cell being either a water hole or a Gd-UO_2 pin cell. The results were compared with reference TRIPOLI-4 values and also with the results of the legacy SG-GR-383g fine-group subgroup method of APOLLO3. The evidence showed that the SG-IR-69g method reached an accuracy similar to the one of the SG-GR-383g method on the multiplication factor, but more importantly, error compensations in space and energy were observed with the SG-IR-69g method. Although the on-the-fly calculation of the mixture PPTs was more expensive than that of the mixture MPTs, the SG-IR-69g was overall more efficient than the SG-GR-383g, even for small motifs of 3 × 3 pin cells, thanks to the decrease in the number of energy groups by more than a factor 5.

Future work is focused on increasing the precision of the SG-IR-69g self-shielding methods. Different improvements are being considered. The calculation method of the IR parameters is currently in preliminary development; it should not only be improved to enforce a better preservation of the reaction rates, but also be extended to a larger energy domain. Another prospect is the refinement of the UFG energy mesh employed in the UFG IHM solver to calculate the effective cross sections of the mixture. The generation of higher-order PPTs should be explored to decrease the errors in the subgroup calculations. Finally, the self-shielding of the transfer cross sections is being considered, as the use of infinitely diluted ones is not appropriate for coarse-group calculations.

Improvements to the implementation of the SG-IR-69g method, such as the parallelization of the UFG IHM calculations, of the PPT calculations, and of the

subgroup calculations, are also being considered in order to reduce the computational time of the SG-IR -69g method.

Acknowledgments

APOLLO3® and TRIPOLI-4® are registered trademarks of CEA Commissariat à l'Energie Atomique et aux Energies Alternatives. We gratefully acknowledge EDF (Electricité de France) and Framatome for their long-term partnership and their support.

We would like to thank Stéphane Mengelle, Mireille Coste-Delclaux, and Cédric Jouanne for their help in generating the multigroup nuclear data libraries required for our calculations, as well as Odile Petit for her guidance in the use of the TRIPOLI-4 code to provide reference calculations.

Disclosure Statement

No potential conflict of interest was reported by the authors.

ORCID

Li Mao http://orcid.org/0000-0002-6540-2620

References

1. P. RIBON and J. M. MAILLARD, "Les Tables de Probabilités. Application au Traitement des Sections Efficaces pour la Neutronique," Technical Report CEA-N-2485, Commissariat à l'Energie Atomique (1986).
2. R. SANCHEZ et al., "APOLLO2 Years 2010," *Nucl. Eng. Technol.*, **42**, *5*, 474 (2010); https://doi.org/10.5516/NET.2010.42.5.474.
3. P. MOSCA et al., "APOLLO3®: Overview of the New Code Capabilities for Reactor Physics Analysis," presented at the Int. Conf. on Mathematics and Computational Methods Applied to Nuclear Science and Engineering (M&C 2023) (2023).
4. M. HALSALL, "The WIMS Subgroup Method for Resonance Absorption," *Trans. Am. Nucl. Soc.*, **72**, 354 (1995).
5. J. CASAL, "HELIOS: Geometric Capabilities of a New Fuel-Assembly Program," *Proc. Int. Topl. Mtg. on Advances in Mathematics, Computations and Reactor Physics*, **2**, 10 (1991).
6. H. G. JOO et al., "Methods and Performance of a Three-Dimensional Whole-Core Transport Code DeCART," *Proc. PHYSOR 2004—The Physics of Fuel Cycles and Advanced Nuclear Systems: Global Developments*, p. 6 (2004).
7. Y. S. JUNG et al., "Practical Numerical Reactor Employing Direct Whole Core Neutron Transport and Subchannel Thermal/Hydraulic Solvers," *Ann. Nucl. Energy*, **62**, 357 (2013); https://doi.org/10.1016/j.anucene.2013.06.031.
8. Y. LIU et al., "Resonance Self-Shielding Methodology in MPACT," presented at the Int. Conf. on Mathematics and Computational Methods Applied to Nuclear Science and Engineering (M&C 2013), American Nuclear Society (2013).
9. J. CHEN et al., "A New High-Fidelity Neutronics Code NECP-X," *Ann. Nucl. Energy*, **116**, 417 (2018); https://doi.org/10.1016/j.anucene.2018.02.049.
10. A. HÉBERT, "A Review of Legacy and Advanced Self-Shielding Models for Lattice Calculations," *Nucl. Sci. Eng.*, **155**, *2*, 310 (2007); https://doi.org/10.13182/NSE06-50.
11. L. MAO, I. ZMIJAREVIC, and K. ROUTSONIS, "Application of the SPH Method to Account for the Angular Dependence of Multigroup Resonant Cross Sections in Thermal Reactor Calculations," *Ann. Nucl. Energy*, **124**, 98 (2019); https://doi.org/10.1016/j.anucene.2018.09.031.
12. M. COSTE-DELCLAUX, "Modélisation du Phénomène d'Autoprotection dans le Code de Transport Multigroupe APOLLO2," PhD Thesis (2006); http://www.theses.fr/2006CNAM0516.
13. M. COSTE-DELCLAUX and S. MENGELLE, "New Resonant Mixture Self-Shielding Treatment in the Code APOLLO2," presented at PHYSOR 2004—The Physics of Fuel Cycles and Advanced Nuclear Systems: Global Developments, Chicago, Illinois (2004).
14. E. BRUN et al., "TRIPOLI-4®, CEA, EDF and AREVA Reference Monte Carlo Code," *Ann. Nucl. Energy*, **82**, 151 (2015); https://doi.org/10.1016/j.anucene.2014.07.053.
15. L. MAO, I. ZMIJAREVIC, and R. SANCHEZ, "A Subgroup Method Based on the Equivalent Dancoff-Factor Cell Technique in APOLLO3® for Thermal Reactor Calculations," *Ann. Nucl. Energy*, **139**, 107212 (2020); https://doi.org/10.1016/j.anucene.2019.107212.
16. E. ROSIER, L. MAO, and L. LEAL, "Dynamic Construction of Physical Probability Tables for Resonant Mixtures," *Proc. ANS M&C 2021—The Int. Conf. on Mathematics and Computational Methods Applied to Nuclear Science and Engineering*, p. 1992 (2021).
17. R. GOLDSTEIN and E. COHEN, "Theory of Resonance Absorption of Neutrons," *Nucl. Sci. Eng.*, **13**, *2*, 132 (1962); https://doi.org/10.13182/NSE62-1.
18. Z. LIU et al., "The Pseudo-Resonant-Nuclide Subgroup Method Based Global-Local Self-Shielding Calculation Scheme," *J. Nucl. Sci. Technol.*, **55**, *2*, 217 (2018); https://doi.org/10.1080/00223131.2017.1394232.

19. D. L. ALDAMA, F. LESZCZYNSKI, and A. TRKOV, "WIMS-D Library Update, Final Report of a Coordinated Research Project," International Atomic Energy Agency (2003).

20. M. LIVOLANT and F. JEANPIERRE, "Autoprotection des Résonances dans les Réacteurs Nucléaires. Application aux Isotopes Lourds," CEA-R-4533, Commissariat à l'Energie Atomique (1974).

21. L. MAO, R. SANCHEZ, and I. ZMIJAREVIC, "Considering the IP-Scattering in Resonance Interference Treatment in APOLLO3®," presented at the ANS M&C2015–Joint Int. Conf. on Mathematics and Computation, Supercomputing in Nuclear Applications, and the Monte Carlo Method (2015).

22. M. COSTE-DELCLAUX, "GALILEE: A Nuclear Data Processing System for Transport, Depletion and Shielding Codes," *Proc. Second Workshop on Nuclear Data Evaluation for Reactor Applications* (2008).

23. J. SUBLET, P. RIBON, and M. COSTE-DELCLAUX, "CALENDF-2010: User Manual," Technical Report, Commissariat a l'Energie Atomique (2011).

24. N. HFAIEDH, "Nouvelle Méthodologie de Calcul de l'Absorption Résonnante," PhD Thesis, Université Louis Pasteur (Sep. 21, 2006).

25. A. HÉBERT and A. SANTAMARINA, "Refinement of the Santamarina-Hfaiedh Energy Mesh Between 22.5 eV and 11.4 keV," presented at the Int. Conf. on the Physics of Reactors, Interlaken, Switzerland, September 14–19, 2008.

26. S. MENGELLE, "Maillage un¡versel à pas constants en léthargie : MUSCLET," Technical Report, Commissariat à l'Energie Atomique (2016).

27. A. C. ALDOUS, "Numerical Studies of the Hydrogen Equivalent of Some Structural Materials in Their Effect on U-238 Resonance Capture," Technical Report AEEW-M 860, Atomic Energy Establishment (1969).

28. E. ROSIER, "Study, Development and Evaluation of the Subgroup Methods Based on the Physical Probability Tables in APOLLO3® for Thermal Reactor Calculations," PhD Thesis, Université Paris-Saclay (2022); https://theses.hal.science/tel-04005789.

29. T. Levy, L. Mao, R. Sanchez, E. Rosier, I. Zmijarevic, S. Mengelle, C. Jouanne, O. Petit, "Comparison of Two Infinite Homogeneous Medium Ultra Fine Group Neutron Slowing-Down Solvers in APOLLO3®," presented at the ANS PHYSOR 2024 - International Conference on Physics of Reactors, San Francisco, CA, USA, April 21 - 24, 2024.

30. A. HÉBERT, *Applied Reactor Physics*, 3rd ed. Presses Polytechnique de Montréal (2020); http://www.presses-polytechnique.ca/fr/applied-reactor-physics-third-edition.

31. E. ANDERSON et al., *LAPACK Users' Guide*, Society for Industrial and Applied Mathematics (1999).

32. O. ABERTH, "Iteration Methods for Finding All Zeros of a Polynomial Simultaneously," *Math. Comput.*, **27**, *122*, 339 (1973); https://doi.org/10.1090/S0025-5718-1973-0329236-7.

33. H. PARK and H. G. JOO, "Practical Resolution of Angle Dependency of Multigroup Resonance Cross Sections Using Parametrized Spectral Superhomogenization Factors," *Nucl. Eng. Technol.*, **49**, *6*, 1287 (2017); https://doi.org/10.1016/j.net.2017.07.015.

34. A. HÉBERT, "The Ribon Extended Self-Shielding Model," *Nucl. Sci. Eng.*, **151**, *1*, 1 (2005); https://doi.org/10.13182/NSE151-1-24.

35. A. YAMAMOTO et al., "Benchmark Problem Suite for Reactor Physics Study of LWR Next Generation Fuels," *J. Nucl. Sci. Technol.*, **39**, *8*, 900 (2002); https://doi.org/10.1080/18811248.2002.9715275.

36. S. SANTANDREA and P. MOSCA, "Linear Surface Characteristic Scheme for the Neutron Transport Equation in Unstructured Geometries," presented at the PHYSOR-2006, ANS Topl. Mtg. on Reactor Physics (2006).

37. A. SANTAMARINA et al., "The JEFF-3.1. 1 Nuclear Data Library," *JEFF Report*, **22**, *10.2*, 2 (2009).